RESEARCH ARTICLE

A Novel Locking Buttress Plate Designed for Simultaneous Medial and Posterolateral Tibial Plateau Fractures: Concept and Comparative Finite Element Analysis

Bangji Yan, MBBS[1], Xiaotao Huang, MM[1], Yingxing Xu, MD[2], Chengshi Zou, MBBS[3]

Department of [1]Orthopaedics and Traumatology and [3]Radiology, Cixi Hospital of Traditional Chinese Medicine, Ningbo and [2]Department of Trauma Center, First Affiliated Hospital of Kunming Medical University, Kunming, China

Objective: The complex tibial plateau fractures involving both medial and posterolateral columns are of frequent occurrence in clinics, but the existing fixation system cannot deal with medial and posterolateral fragments simultaneously. Therefore, a novel locking buttress plate named as medial and posterior column plate (MPCP) was designed in this study to fix the simultaneous medial and posterolateral tibial plateau fractures. Meanwhile, the comparative finite element analysis (FEA) was conducted to investigate the discrepancy between MPCP and traditional multiple plates (MP + PLP) in their biomechanical characteristics.

Methods: Two 3D finite element models of simultaneous medial and posterolateral tibial plateau fracture fixed with MPCP and MP + PLP system, respectively, was constructed. To imitate the axial stress of knee joint in ordinary life, diverse axial forces with 100, 500, 1000, and 1500 N were applied in the two fixation models, and then the equivalent displacement and stress nephograms and values were obtained.

Results: The similar trend of displacement and stress increasing with the loads was observed in the two fixation models. However, several heterogeneities of displacement and stress distribution were found in the two fixation models. The max displacement and von Mises stress values of plates, screws, and fragments in the MPCP fixation model were significantly smaller than that in the MP + PLP fixation model, except for the max-shear stress values.

Conclusion: As a single locking buttress plate, the MPCP system showed the excellent benefit on improving the stability of the simultaneous medial and posterolateral tibial plateau fractures, compared with the traditional double plate fixation system. However, the excessive shear stress around screw holes should be paid attention to prevent trabecular microfracture and screw loosening.

Key words: Biomechanics; Finite Element Analysis; Fixation; Locking Buttress Plate; Tibial Plateau Fracture

Introduction

As a frequently presented injury around the knee joint, tibial plateau fractures account for 9.2% of all tibia fractures and are generally considered to be caused by severe trauma caused by the splitting, displacement, and even collapse of the articular surface.[1,2] Therefore, open reduction and internal fixation (ORIF) are usually recommended for the fixation of tibial plateau fractures to restore the flatness of the articular surface and to reduce the occurrence of complications, such as pain, stiffness, and traumatic arthritis of the knee.[3–5]

The Schatzker classification system is widely used for tibial plateau fractures, and fractures are classified into six types based on whether the medial and lateral tibial plateau

Address for correspondence Xiaotao Huang, MM, Department of Orthopaedics and Traumatology, Cixi Hospital of Traditional Chinese Medicine, Ningbo, Zhejiang 315300, China. Email: huangdoctor1234@sina.com
Received 29 August 2022; accepted 23 December 2022

are involved.[6] Among them, medial tibial plateau fractures belong to the type IV in Schatzker classification system, are mostly the result of high-energy injuries, and are usually unstable, although they account for only 14.5% of tibial plateau fractures.[6,7] Medial tibial plateau fractures by themselves are not common and are often accompanied by other injuries, especially posterolateral plateau fractures. Unfortunately, this complex type of tibial plateau fracture has not been described in the Schatzker classification system.

To our knowledge, posterolateral plateau fractures are included in the three-column classification system, which was first presented in 2010 and categorizes factures based on whether they affect the medial, lateral, and posterior columns using the axial computed tomography (CT) images.[8] Compared with the Schatzker classification system, this classification system creatively depicts the posterior column fractures of tibial plateau, and emphasizes the injury characteristics and fixation of this type of fractures, providing valuable guidance for the fixation of complex tibial plateau fractures.[8,9] In general, the posterior column fractures of tibial plateau are mostly attributed to the shear stress exerted in the knee flexion position, and is usually accompanied by posterolateral fragments on the coronal plane.[9]

Based on the three-column classification system, medial combined with posterolateral tibial plateau fractures are classified as two-column fractures (medial and posterior columns).[8,9] Therefore, it is challenging to adequately stabilize separated or collapsed two-column fragments using a single plate fixation due to the limitation of existing plate-screw systems. Thus, multiple plates are often used for this type of fractures in a clinical setting, which leads to an increase in costs, prolonged operation times, and the risk of developing infections.

Here, we performed a study with the aims to: (1) design a novel locking buttress plate to replace traditional multiple plates used to provide the support and fixation effects for medial and posterior column fractures of the tibial plateau and named as "medial and posterior column plate (MPCP)" system; (2) conduct the comparative finite element analysis (FEA) to investigate discrepancies in the biomechanical characteristics, including fixation strength, stress, and displacement distribution, between MPCP and traditional multiple plates; and (3) offer theoretical evidence for the future clinical application of MPCP system.

Materials and Methods

MPCP System Design Concept

The MPCP system was designed as a T-shaped structure based on the anatomy of the proximal posterior tibia, and was composed of proximal transverse and distal shaft sections. The proximal transverse section extended from the posteromedial column to the posterolateral column of the tibial plateau, and was designed using multiaxial locking screw holes (the screw diameter was 3.5 mm) to facilitate screw placement based on the specific shapes of the fragments. The distal shaft section included one compression screw hole (the screw diameter was 5.0 mm) attached to the plate on the surface of the bone, and included two or three locking screw holes (the screw diameter was 5.0 mm), and one of the screws were designed to be a kick-stand screw to provide support. The MPCP system was composed of titanium alloy plate and screws, which was provided by Guangci Medical Instrument limited company (Zhejiang, China). The detailed characteristics of the MPCP system are shown in Figure 1.

Finite Element Model Construction

The CT scan data conducted through 1.0 slice thickness for the full length of right tibiofibula on a healthy adult male (35 years old, 170 cm in height, 60 kg body weight) without comorbidities, such as degeneration, osteoarthritis, instability, and fractures, was obtained and used to construct a three-dimensional tibiofibula finite element model using Mimics software (v21.0, Materialize Company, Belgium). Subsequently, the initial model was further improved using Geomagic Studio Software (v2017, 3D system Inc., Rock Hill, USA). In addition, the 3D models of all screws and plates were created using computer-aided design (CAD) software based on the following parameters: (1) the MPCP system was designed with 12 locking screw holes (proximal: eight screws with a diameter of 3.5 mm; distal: four screws with a diameter of 5.0 mm), and detailed characteristics are shown in Figure 2A,C; (2) the medial T-shaped plate was composed of seven locking screw holes (proximal: two screws with diameter of 5.0 mm; distal: five screws with diameter of 5.0 mm), and detailed characteristics are shown in Figure 2D,H; (3) the inclined T-shaped plate was composed of eight locking screw holes (proximal: four screws with a diameter of 2.7 mm; distal and four screws with a diameter of 3.5 mm) as previously described[7,10] and detailed characteristics are shown in Figure 2G,I.

In addition, a medial and posterolateral tibial plateau fracture model was created using CAD software as previously reported.[7,10] The detailed method was as follows:

1. the medial plateau fracture was created by extending the medial edge of tibial tuberosity 5 cm distal to the medial plateau (Figure 2B,E).
2. the posterolateral tibial plateau fracture was constructed by including an angle of 232° between line A and B. Specifically, line A was defined as the connecting line between the middle point of the posterior cruciate ligament (PCL) insertion on the tibial plateau and the medial 1/3 point of the tibial tuberosity, and B was defined as a connecting line between the two sides of the fracture line (Figure 2B,E).

Subsequently, the fracture fixation models were constructed by placing the plate-screw systems in the proper position on the tibial plateau, and dividing them into two

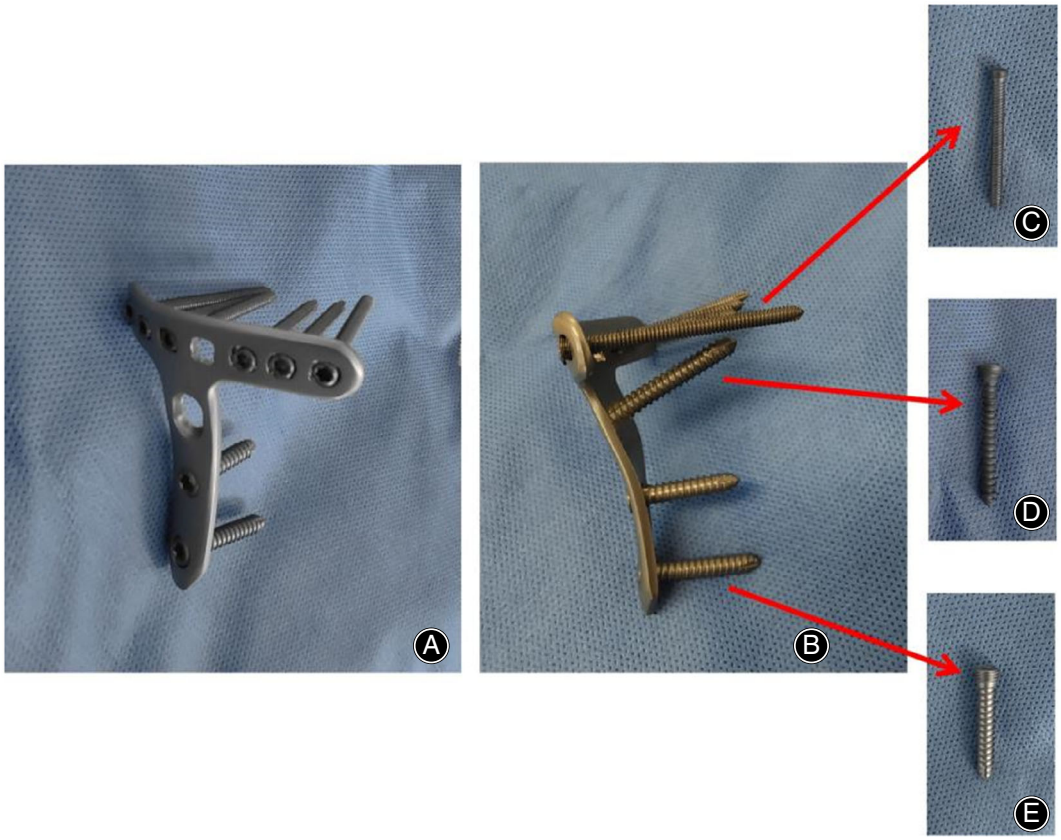

FIGURE 1 Representative images in the MPCP system. (A) Oblique photographs showing the shape of MPCP and screw distribution. (B) Lateral photograph showing the directions and types of screws. (C) Multiaxial locking screw with a diameter of 3.5 mm. (D) Compression screw with diameter of 5.0 mm, which can be replaced with locking screw as a kick-stand screw based on intraoperative needs. (E) Locking screw with a diameter of 5.0 mm

groups: (1) the medial and posterolateral plateau fractures were fixed with MPCP (MPCP) (Figure 2B); (2) the medial plateau fracture was fixed with the medial T-shaped plate, and the posterolateral plateau fracture was fixed with the inclined T-shaped plate (MP + PLP) (Figure 2E).

Furthermore, all models were re-meshed and the finite element models were established using ANSYS software (17.0 version, Ansys Company, USA). The selection of unit type was conducted using the C4H10 higher order element, and detailed information of the two groups are shown in Figure 2J,K.

Material Properties

The materials used in all implants and bones were assumed to be isotropic, homogeneous, elastic, and linear. Based on material properties reported in previous studies,[7,10,11] elastic modulus of 110,000 MPa, 14,000 MPa, and 700 MPa and a Poisson ratio of 0.3, 0.3, and 0.2 were assigned to the titanium alloy plate-screw system, cortical bone, and trabecular bone in the finite element models, respectively.

Loading and Boundary Conditions

Under restraint, the distal tibia and fibula (Figure 3A,B) of the medial tibial plateau were loaded with axial forces of 100, 500, 1000, and 1500 N with a distribution of 60%, while the lateral tibial plateau was loaded with an axial force with a distribution of 40% (Figure 3C–E).[10,12] The locking screw mechanism was simulated by assuming that the contact surfaces between the plates and screws shared common nodes. The contact between the implants and bones were assumed to be direct, and a frictional coefficient of 0.4 was assigned to the contact surfaces between them.[13]

Finite Element Analysis

ANSYS software was used for the finite element analysis to obtain the displacement and stress nephogram of the two fracture fixation models. In addition, from right to left, anterior to posterior, and distal to proximal were defined as positive directions of the X, Y, and Z axes, respectively. The detailed displacements in the different axes were obtained. Meanwhile, the max von Mises stress and max-shear stress values of the two fixation models were calculated.

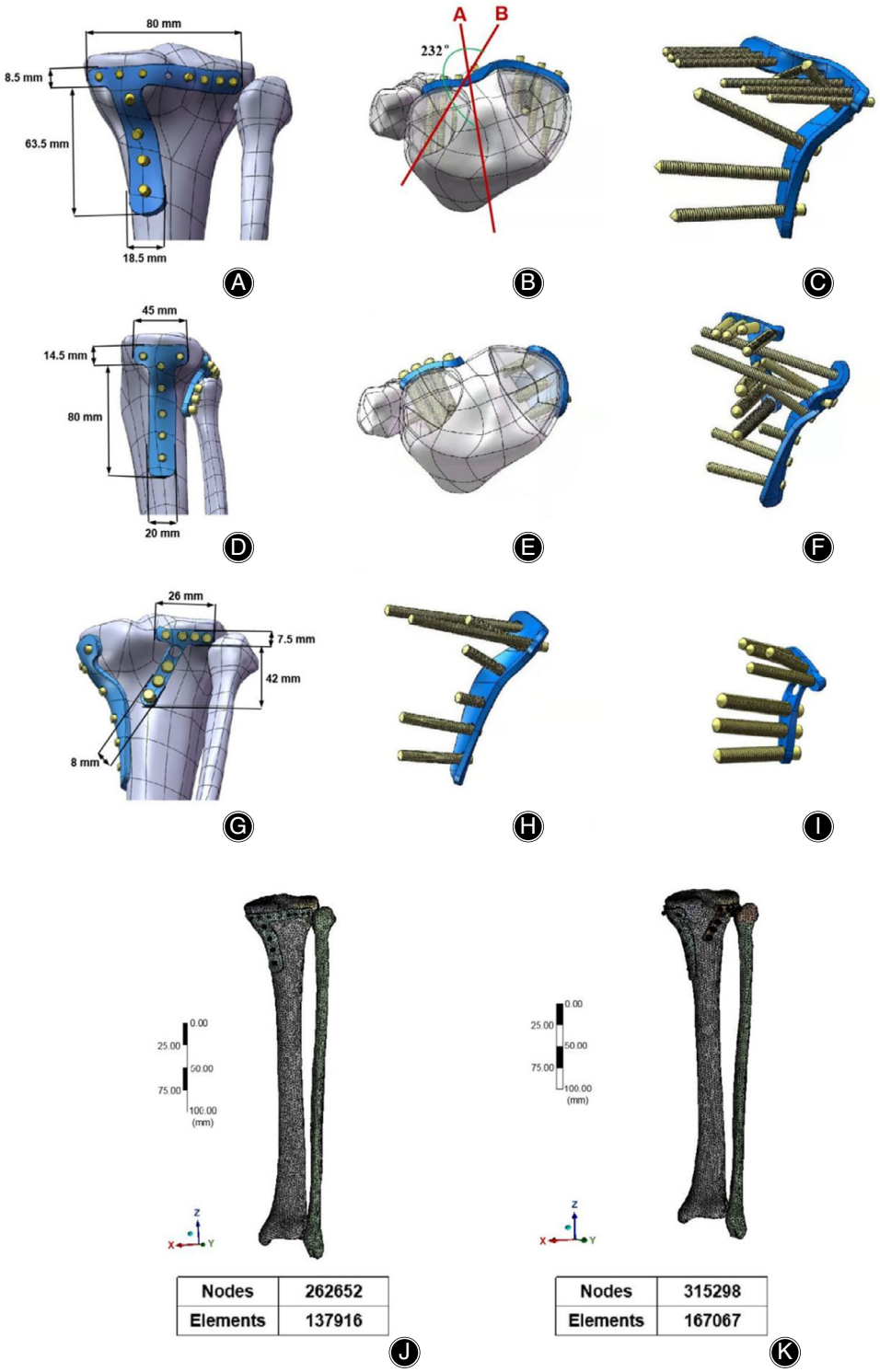

FIGURE 2 Finite element model construction. (A) Details on the MPCP system model. (B) Details of simultaneous medial and posterolateral tibial plateau fractures model fixed with MPCP system. (C) General appearance of MPCP system model. (D) Details on the medial T-shaped plate model. (E) Details on simultaneous medial and posterolateral tibial plateau fractures model fixed using the MP + PLP system. (F) General appearance of the MP + PLP system model. (G) Details on the inclined T-shaped plate model. (H) General appearance of the medial T-shaped plate model. (I) General appearance of the inclined T-shaped plate model. (J) The selection of a unit type for the MPCP fixation model. (K) The selection of a unit type for the MP + PLP fixation model

Results

Displacements in the Two Fixation Models

Details on displacements, including the maximal and minimal values in the X, Y, and Z axes, in the two fixation models under axial forces of 100, 500, 1000, and 1500 N are displayed in Table 1. The analysis showed a similar trend of displacement along with an increase in the loads observed in both fixation models. Therefore, the representative equivalent maps of 1500 N in the two fixation models are shown in

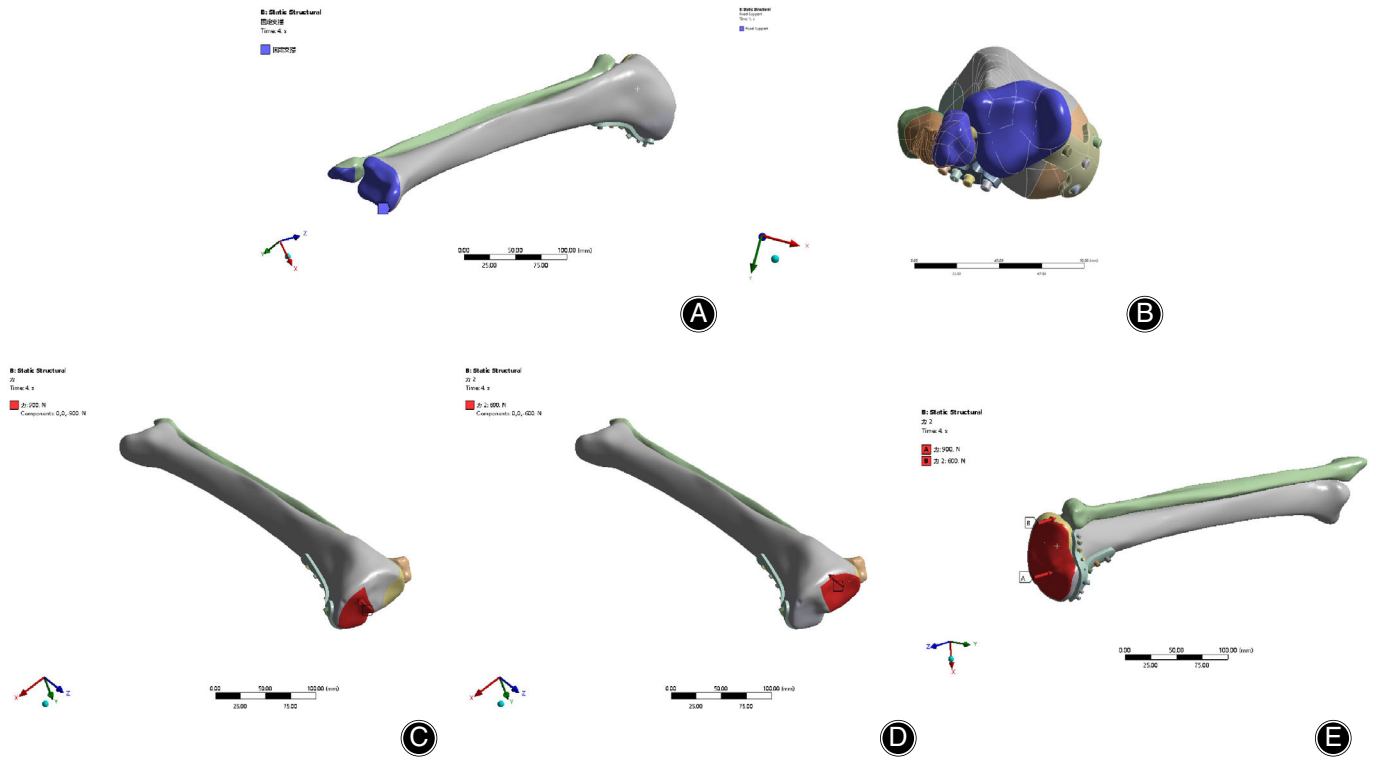

FIGURE 3 Loading and boundary conditions. (A and B) Boundary conditions used for restraining the distal tibia and fibula. (C) Loading condition of the medial tibial plateau. (D) Loading condition of the lateral tibial plateau. (E) Loading condition of the entire tibial plateau

Figure 4. Heterogeneity in displacement distribution was observed in the 3D space on different axes in both the MPCP and MP + PLP fixation models. Specifically, the maximal overall displacement and that of the X-axis was concentrated in the proximal tibia (Figure 4A,B,E,F), whereas, maximal displacement in the Y-axis and Z-axis was concentrated in the distal tibiofibula and proximal fibula, respectively (Figure 4C,D,G,H). Moreover, it was remarkable that the maximal overall displacement values and that of the X-axis and Z-axis under different axial forces of 100, 500, 1000, and 1500 N in the MPCP fixation model were significantly lower than that in the MP + PLP fixation model, indicating that the MPCP system showed better fixation strength in the medial and posterolateral tibial plateau fracture model, compared with MP + PLP system (Table 1).

Stress Distributions in the Two Fixation Models

Details on stress values including max von Mises stress and max-shear stress in the two fixation models under different axial forces of 100, 500, 1000, and 1500 N are listed in Table 2. Similar to the trend of maximal displacement, the maximum stress on the plates, screws, fragments, and tibia shaft increased along with the increase in load in a roughly linear manner. Therefore, the equivalent stress nephograms with a load of 1500 N on the two fixation models are presented in Figure 5.

The overall stress distribution showed that maximum stress was concentrated in the junction between the plates and fracture lines, as well as in the medial area of the tibial shaft below the plate systems (Figure 5A1,A2). For the stress distribution on the bone, the maximum stress on the bone was located on the area around the fracture line under the plate and the transitional area between the distal plate and bone (Figure 5B1,B2).

However, there were some differences in the specific stress distribution characteristics between the two fixation models. Generally, the maximum stress distribution on the plate is concentrated on the plate area around the fracture lines. In details, the maximum stress concentration area could be observed around the first and second screw holes in the distal shaft of the plate, as well as the junction between the posterolateral fracture line and proximal transverse area of plate in the MPCP fixation model. In comparison, in the MP + PLP fixation model, the maximum stress was concentrated around the first and the second screw holes in the distal shaft of the plate in both the medial T-shaped plate and the inclined T-shaped plate (Figure 5C1,C2). In terms of stress distribution in the screws, maximum stress in both two fixation models was concentrated in the plate-screw binding area and trabecular bones surrounding the screw holes. However, several stress concentration areas were observed around the screws of the proximal transverse

TABLE 1 Displacement values of two fixation models

		MPCP				MP + PLP			
Load (N)		100	500	1000	1500	100	500	1000	1500
Overall displacement (mm)		0.11867	0.59255	1.1836	1.7736	0.12253	0.61267	1.2251	1.8371
X axis (mm)	max	0.083944	0.41947	0.83853	1.2573	0.11973	0.59863	1.197	1.7949
	min	−0.003769	−0.018847	−0.037699	−0.056555	−0.0013161	−0.0065834	−0.013171	−0.019762
Y axis (mm)	max	0.00029294	0.0014645	0.0029287	0.0043928	0.00020649	0.0010325	0.0020653	0.0030981
	min	−0.0797	−0.39774	−0.79427	−1.19	−0.031404	−0.1578	−0.31391	−0.469
Z axis (mm)	max	0.0085913	0.042641	0.084896	0.12704	0.012293	0.061629	0.10497	0.18565
	min	−0.03785	−0.18906	−0.37758	−0.56556	−0.042174	−0.21085	−0.35838	−0.632

section of the plate in the MPCP fixation model, compared with the MP + PLP fixation model (Figure 5D1,D2). Nonetheless, it is noteworthy that the maximum von Mises stresses of the plate and screws under different axial forces in the MPCP fixation model were significantly lower than that of the MP + PLP fixation model (Table 2).

In addition, the fracture fragments were divided into medial and posterolateral sections to further investigate the stress distribution of each fragment. In the MPCP fixation model, the maximum stress on the medial fragment was concentrated in the junction between the medial inferior fracture line and plate, as well as in the crossing of the platform fracture line and multiple screws (Figure 5E1–E3). However, a significant stress concentration area was not found on the posterolateral fragment (Figure 5F1–F3). In the MP + PLP fixation model, the maximum stress of medial fragment also was concentrated in the junction between the medial inferior fracture line and plate, but an obvious stress concentration area was not observed in the platform fracture line due to the non-crossing fixation of multiple screws (Figure 5G1–G3). In addition, the maximum stress in the posterolateral fragment in this fixation model was located further above the proximal tibiofibular syndesmosis, compared with the MPCP fixation model (Figure 5H1–H3).

Furthermore, as shown in Figure 6A, the shear stresses of the tibia and fibula in the two fixation models were mainly concentrated at the junction between the fracture lines and the plates, as well as between the bone and the plates. The shear stress distribution of the two fragments in the two fixation models showed similar characteristics and were located at the junction between the fracture lines and the plates, as well as in the trabecular bones around the screw holes (Figure 6B). However, the maximum shear stress values in both the tibiofibula and the two fragments under different axial forces in the MPCP fixation model were significantly higher than that of the MP + PLP fixation model (Table 2).

Relationship between Max-Shear Stress Surrounding Screw Holes and Trabecular Bone Strength

To investigate the potential risk of trabecular fractures in the two fixation models, the max shear stress values of the trabecular bones under different loads: 100, 500, 1000, 1500, 2000 N, were recorded. As shown in Figure 7, the max-shear stresses of the trabecular bones surround screw holes in the two fixation models increased along with the increase in load in a roughly linear manner. Notably, all the max-shear stress values in the MP + PLP fixation model were within the safe range of trabecular bone shear strength (2.4–5.8 MPa),[14] when the various knee joint movements included in this study were simulated (60 kg in body weight), including standing on two legs (100% of body weight, 600 N), flexion motions (220%–250% of body weight, 1320–1560 N), standing on one leg (270% of body weight, 1620 N), and walking up and down stairs (310%–350% of body weight, 1860–2100 N).[15] However, the max-shear stress values under different

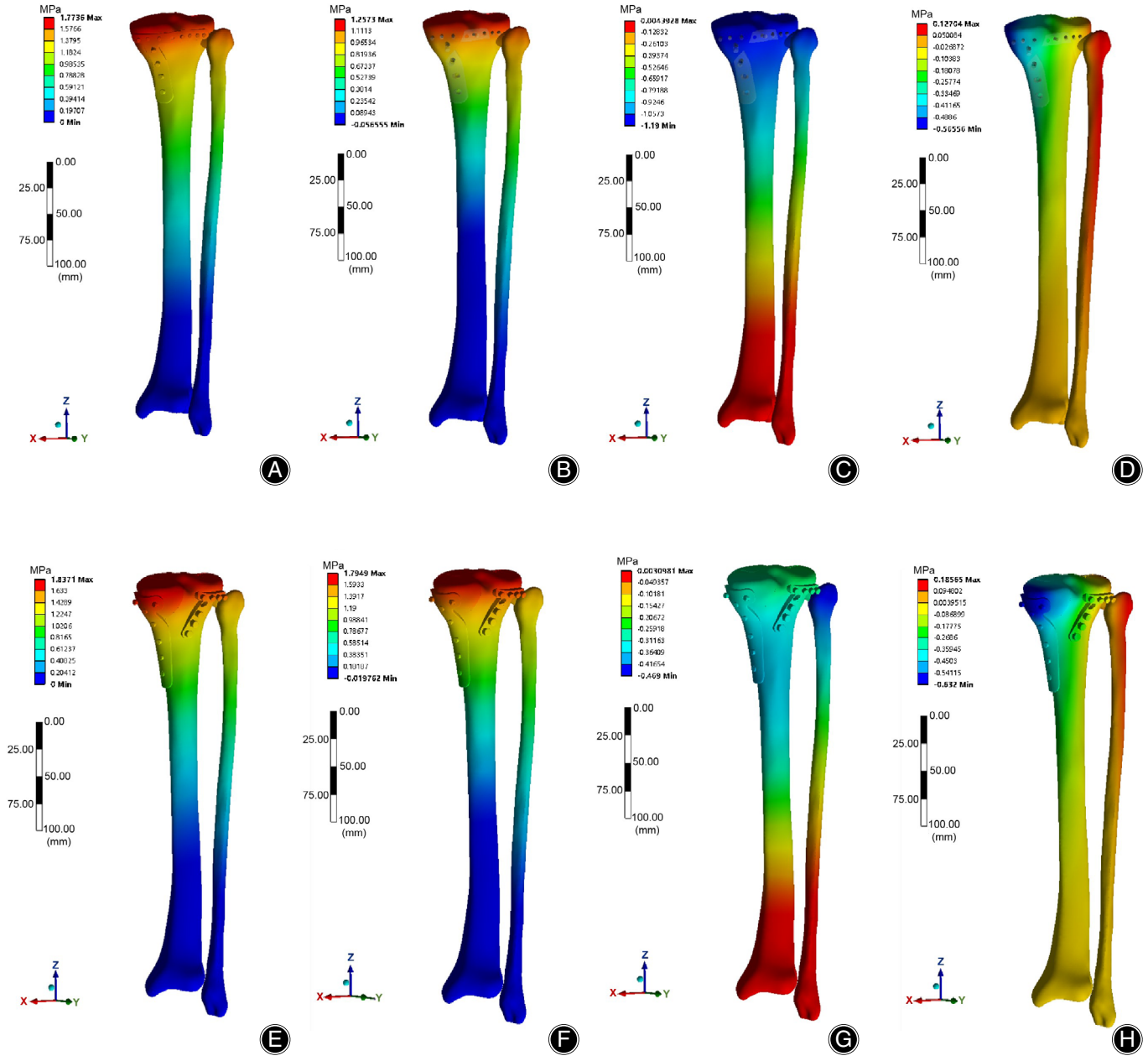

FIGURE 4 Displacement distribution of the two fixation models. (A) Overall displacement distribution of the MPCP fixation model. (B) Displacement distribution of MPCP fixation model on the X-axis. (C) Displacement distribution of the MPCP fixation model on the Y-axis. (D) Displacement distribution of the MPCP fixation model on the Z-axis. (E) Overall displacement distribution of the MP + PLP fixation model. (F) Displacement distribution of the MP + PLP fixation model on the X-axis. (G) Displacement distribution of the MP + PLP fixation model on the Y-axis. (H) Displacement distribution of the MP + PLP fixation model on the Z-axis

loads in the MPCP fixation model were significantly higher than that in the MP + PLP fixation model. Therefore, the max-shear stress values of the trabecular bones surrounding the screw holes in the MPCP fixation model were out of the safe range for trabecular bone shear strength, when the above mentioned movements were simulated, except for standing on two legs.

Discussion

A novel locking buttress plate named "medial and posterior column plate (MPCP)" was designed in this study to treat the simultaneous medial and posterolateral tibial plateau fractures. Based on the biomechanical finite element analysis, we found that the MPCP system could provide more convenient fixation for posterolateral fragments, the

TABLE 2 Stress values of two fixation models

		MPCP				MP + PLP			
Load (N)		100	500	1000	1500	100	500	1000	1500
Max von Mises stress (MPa)	Plate	2.5819	12.916	25.79	38.645	4.5327	22.41	44.602	66.615
	Screws	3.9582	19.611	38.533	56.779	5.3982	26.74	54.583	83.109
	Medial fragment	1.0073	4.9676	10.197	16.169	1.2138	6.0787	12.115	18.066
	Posterolateral fragment	0.7226	3.5685	7.1195	10.658	1.0487	5.1386	10.053	14.702
Max-shear stress (MPa)	Two fragments	0.50273	2.4809	4.8629	7.1944	0.31938	1.5632	3.0559	4.4649
	Tibia and fibula	1.3709	6.8085	13.431	19.836	0.72795	3.6315	7.2303	10.768

smaller displacement and stress of fragments, and the better stability of fractured bones, compared with the traditionally used double plate fixation system.

Challenges of Simultaneous Medial and Posterolateral Tibial Plateau Fractures

Considering the location of fracture lines, the number of fragments, fracture stability, and the degree of comminution, tibial plateau fractures can be divided into simple and complex types. Along with the rapid development of the economy, high-energy injuries have been found to occur more frequently, and have also led to the significant increase in complex tibial plateau fractures. According to the clinical observations, the characteristics of this type of fracture are not only reflected in complex injury mechanisms, comminuted fractures, displaced and collapsed intra-articular fragments, but also in various other injury sites. Among complex tibial plateau fractures, injuries that involve both medial and posterolateral columns are more commonly reported in a clinical setting. Based on injury features, splitting medial fractures and collapsed posteriorlateral fractures are often observed in this type of damage.[9] Thus, reliable medial fixation and posterolateral support are usually required to provide strong fracture stability. To our knowledge, existing methods of internal fixation cannot be used to treat simultaneous medial and posterolateral fragments. Therefore, multiple plates fixation is widely used for this type of fracture (Figure 8). However, attention should be paid to problems caused by multiple plates fixation, such as rising costs, prolonged operation duration, and the risk of developing infections.

Design Concept of the MPCP System

The MPCP system was anatomically designed and placed in the posteromedial area of the proximal tibia, while the proximal transverse section of the MPCP system was developed to fix the entire posterior column of the tibial plateau. Notably, it is usually difficult to expose the posterolateral column using traditional surgical incisions, resulting in inconvenience in inserting screws to fix the posterolateral fragments. To address this, the proximal transverse section was designed by adding multiaxial locking screw holes as it is not only conducive to the placement of posterolateral screws, but also increased the fixed range of the medial screws to stabilize the medial column. In this case, a reversed L-shaped incision described by Luo et al.[8] is recommended, so that no additional posterolateral incision is required to avoid irritation of the nervus peroneus communis. Furthermore, the screw diameter was 3.5 mm, which was beneficial for providing more space for the placement of multiple screws, and the distal shaft of the MPCP system was designed with one compression screw hole to attach the plate to the surface of bone and a kick-stand screw hole to provide support. Moreover, additional attention needs to be paid to the risks associated with screw collisions. For the traditional double plate system, it is usually necessary to place the posterolateral plate first, and then the medial plate. For the MPCP system, a reasonable screw placement sequence is also required to avoid screw collision. In detail, the subsequent placement of the posterolateral screw is often recommended after the compression screw is placed, so that the screw collisions can be effectively avoided by controlling the screw length when the posterolateral screw is placed.

Characteristics of Displacement in the 3D Space in the Two Fixation Models

To further verify the validity of the MPCP system for the fixation of simultaneous medial and posterolateral tibial plateau fractures, a biomechanical finite element analysis to compare the MPCP system and the traditional multiple plate fixation was performed in this study. First, displacement in the 3D space (X, Y, and Z axes) was analyzed in the two fixation models under different loads. As shown in Table 1, the maximal displacement of the MP + PLP fixation model on the X-axis was significantly greater than that of MPCP fixation model and was mainly located on the proximal tibia. Based on the characteristics of the fracture model, displacement on the X-axis represents the degree of displacement of the medial and posterolateral fragments under shear stress in the left and right directions. In addition, the maximal displacement of the two fixation models on the Y-axis (in the anterior and posterior directions) was located in the lower tibia and was relatively slight, although the maximal displacement values in the MPCP fixation model were higher than that of the MP + PLP fixation model. These findings demonstrate that the MPCP system could provide better stability for the

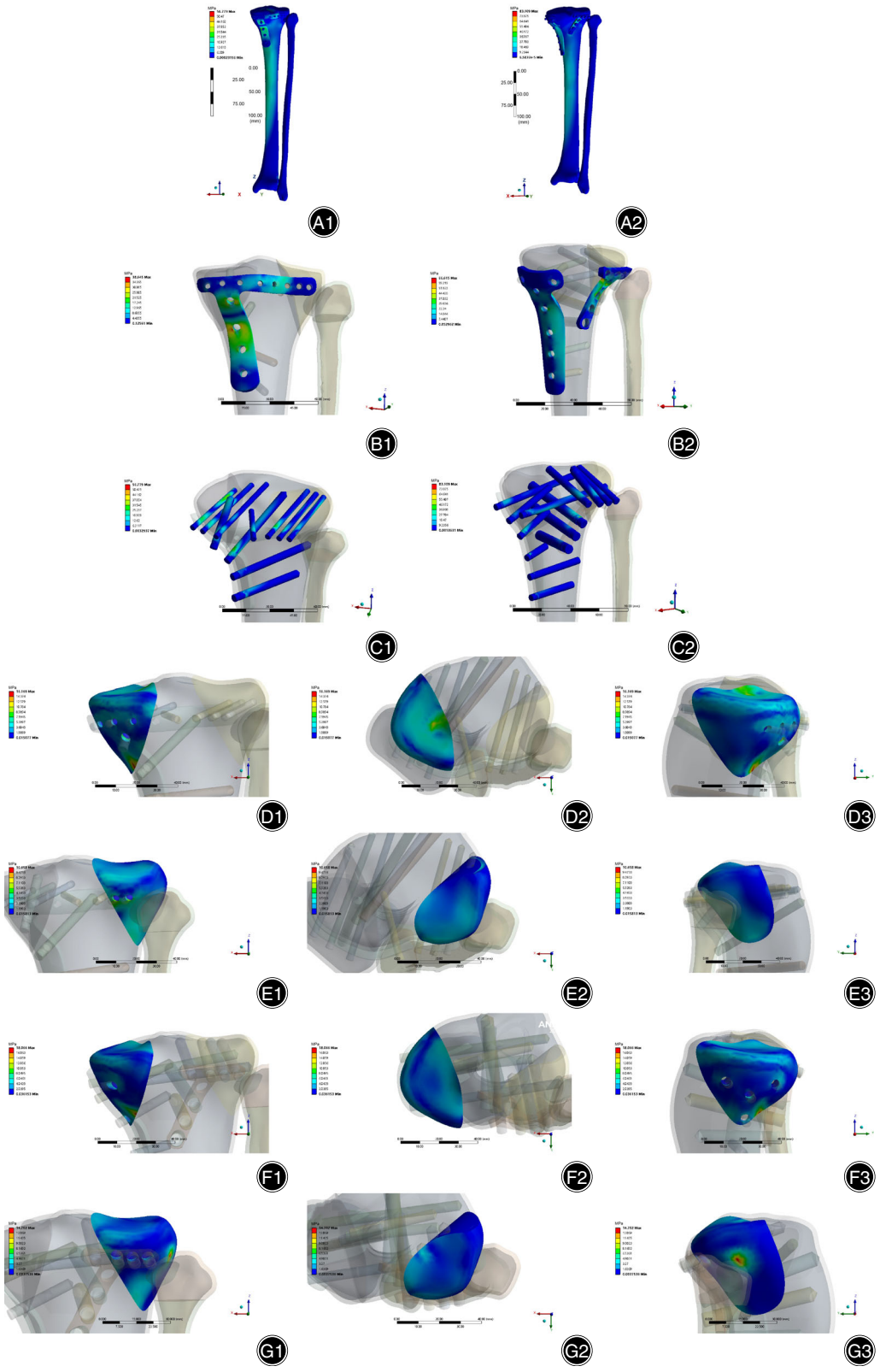

FIGURE 5 Legend on next coloumn.

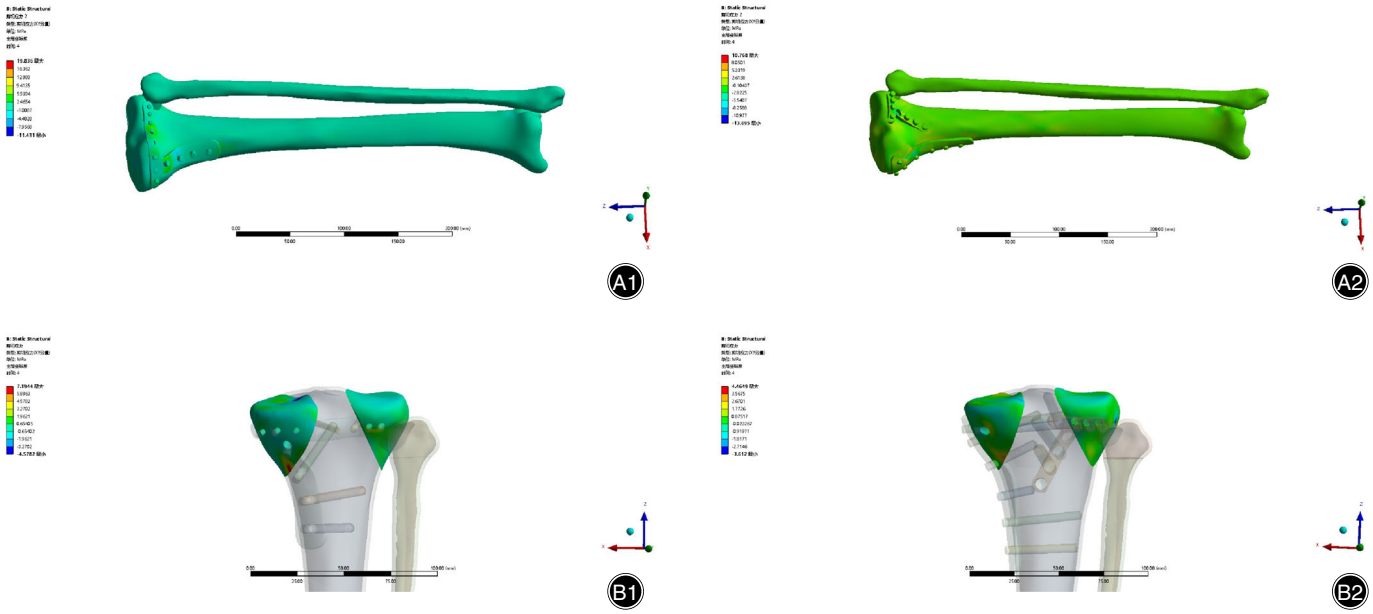

FIGURE 6 The shear stress distributions in the two fixation models. (A1) The shear stress distributions on the tibia and fibula in the MPCP fixation model. (A2) The shear stress distributions on the tibia and fibula in the MP + PLP fixation model. (B1) The shear stress distributions on fragments in the MPCP fixation model. (B2) The shear stress distributions on fragments in the MP + PLP fixation model

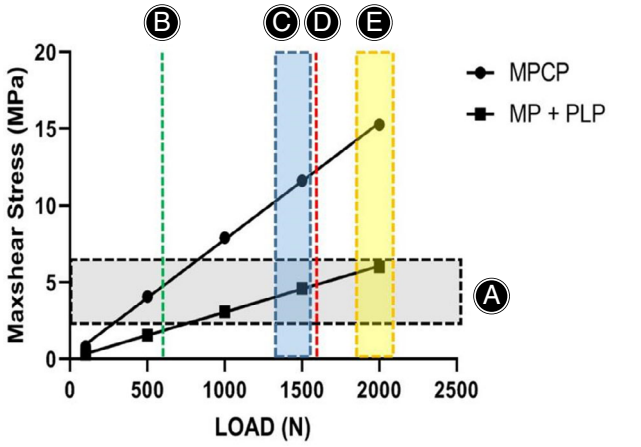

FIGURE 7 The relationship between max-shear stress surrounding the screw holes and the trabecular bone strength. (A) The safe range of the trabecular bone shear strength (2.4–5.8 MPa). (B) Load while standing on two legs standing (600 N). (C) Load range of the flexion motions (1320–1560 N). (D) Load while standing on one leg (1620 N). (E) Load range while walking up and downstairs (1860–2100 N)

fixation of simultaneous medial and posterolateral tibial plateau fractures. It should be noted that the larger maximal displacement values on the Z-axis were observed in the MP + PLP fixation model rather than in the MPCP fixation model, and were concentrated in the proximal fibula, indicating that greater fixation strength was required by the MP + PLP fixation system, compared with the MPCP system in the presence of a proximal fibula fracture.

Characteristics of Stress Distribution in the Two Fixation Models

Furthermore, the characteristics of stress distribution on the bone, the plates, the screws, and fracture fragments in the two fixation models were recorded. Among them, von Mises stress was used to evaluate the yield failure of the plates and screws. In general, the maximum stress distribution on the plates and screws were concentrated on the area around the fracture lines and the plate-screw binding area in the two fixation models. However, under different axial forces of 100, 500, 1000, and 1500 N, the max von Mises stress of the plate and screws in the MPCP fixation model was

FIGURE 5 The von Mises stress distributions of the two fixation models. (A1) Overall von Mises stress distribution of the MPCP fixation model. (A2) Overall von Mises stress distribution of the MP + PLP fixation model. (B1) The von Mises stress distribution on the plates of the MPCP fixation model. (B2) The von Mises stress distribution on the plates of the MP + PLP fixation model. (C1) The von Mises stress distribution on the screws of the MPCP fixation model. (C2) The von Mises stress distribution on the screws of the MP + PLP fixation model. (D1–D3) The von Mises stress distribution on the medial fragment in the coronal, transverse, and sagittal positions of the MPCP fixation model. (E1–E3) The von Mises stress distribution on the posterolateral fragment in the coronal, transverse, and sagittal positions for the MPCP fixation model. (F1–F3) The von Mises stress distribution on the medial fragment in the coronal, transverse, and sagittal positions for the MP + PLP fixation model. (G1–G3) The von Mises stress distribution on the posterolateral fragment in the coronal, transverse, and sagittal positions in the MP + PLP fixation model

FIGURE 8 Representative images of a patient with simultaneous medial and posterolateral tibial plateau fractures. (A) Preoperative X-ray showing the general shape of the fracture. (B) Preoperative CT imaging showing the details of the fracture with significant collapse or syntripsis of the articular surface. (C) Postoperative X-ray showing multiple plates fixation

significantly lower than that in the MP + PLP fixation model, demonstrating a lower probability of yield failure in the MPCP system, compared with the MP + PLP system. Notably, although all max von Mises stress values in the two fixation models were far lower than the maximum resistance strength of the titanium alloy (795 MPa),[14] these results were obtained only under instantaneous loading, while fatigue failure caused by long-term loading was not evaluated in this study.

Moreover, maximum stress on the medial fragments were mainly concentrated at the junction between the tibial shaft fracture lines and plates in both fixation models, which was the result of resisting the axial load applied to the medial fragments. In addition, the maximum stress concentration on the crossing between the medial platform fracture line and multiple screws was found in the MPCP fixation model. Therefore, the shaft of the MPCP system was placed in the posteromedial area of the tibial plateau, while cross fixation was speculated to occur between the shaft section screws and the transverse section screws. It was reported that the extrusion motion produced by cross fixation could provide greater compression on the medial fragment to improve fracture stability and promote bone healing.[13] In comparison, the medial T-shaped plate was placed on the medial tibial plateau, and stress concentrated on the platform caused by cross fixation of screws was not observed in the MP + PLP fixation model.

However, maximum stress was also concentrated on the posterolateral fragment above the proximal tibiofibular syndesmosis in the MP + PLP fixation model, which was speculated to be the result of restriction between the inclined T-shaped plate and proximal fibula. Remarkably, the max-shear stress values of the two fragments and tibiofibula under different axial forces in the MP + PLP fixation model were lower than that of the MPCP fixation model, showing the inherent advantage of fixation using double plates. Whereas, lower max von Mises stress values of both the medial and posterolateral fragment were observed in the MPCP fixation model, indicating that simultaneous fixation of the two fragments by the MPCP system led to stress dispersion.

Characteristics of Max-Shear Stress in the Two Fixation Models

The max-shear stress was usually estimated for the bones to illustrate the danger of trabecular microfractures, which may lead to screw loosening and further ORIF failure.[10] As shown in Figure 6, the greatest max-shear stresses in the facture fragments of the two fixation models were discovered around the fracture surfaces in the screw holes. Therefore, the relationship between max-shear stress surrounding the screw holes and the trabecular bone strength were explored to evaluate the potential risk of trabecular fractures in both fixation models. It was reported that the shear strength of the trabecular bone ranged from 2.4 to 5.8 MPa,[14] and the axial load on the knee joint varied from 100%–360% of body weight during daily activities.[15] Thus, axial force of 100, 500, 1000, 1500, 2000 N were applied in the experiment to simulate various movements of the knee joint, such as standing on two legs (600 N), flexion motions (1320–1560 N), standing on one leg (1620 N), and walking up and down stairs (1860–2100 N), since the body weight of patient used in this study was 60 kg. As shown in Figure 7, the max-shear stress values of the trabecular bones surrounding the screw holes under different loads in the MPCP fixation model were significantly higher than that of the MP + PLP fixation model, and were out of the safe range of trabecular bone shear strength (2.4–5.8 MPa), when the various movements of the knee joint were simulated, except for standing on two legs. In comparison, double plate fixation (MP + PLP fixation system) exhibited a lower risk of trabecular microfractures. To be able to provide good fracture stability, the shear stresses of trabecular bones surrounding the screw holes under the same load in a single plate fixation system are usually larger than that of a double plate fixation system, which may be due to stress being concentrated on the screws caused by single plate fixation. In this case, it was suggested that patients treated using the MPCP system should avoid early weight-bearing after operation.

Strengths and Limitations

This study have confirmed the superiority of MPCP system in fixation of simultaneous medial and posterolateral tibial plateau fractures based on the systematic biomechanical finite element analysis. However, our study still encounters some limitations. First, the fracture model in this study was constructed based on healthy people, which is not exactly the same as the clinical fracture patients. In addition, the excessive shear stresses of trabecular bones around the screw holes was found in the MPCP system, which requires the patient to delay postoperative weight bearing. Moreover, the results of this study are only from biomechanical analysis, and there is no evidence of cadaveric research and clinical application, which is expected to be improved in our future studies.

Conclusion

As a single locking buttress plate, the MPCP system showed some advantages in the simultaneous medial and posterolateral tibial plateau fracture model, compared with the traditionally used double plate fixation system. The design of multiaxial locking screw holes in the proximal transverse section of the plate was beneficial for the placement of screws for the fixation of posterolateral fragments. Furthermore, the cross fixation of multiple screws provided by this fixation system could reduce displacement and stress of the fragments, and improve the stability of the fractured bones. However, attention should be paid to the excessive shear stress around the screw holes to prevent trabecular microfractures and screw loosening.

Author Contributions

Material preparation, data collection and analysis were performed by Bangji Yan and Yingxing Xu. The first draft of this manuscript was written by Bangji Yan. Study conception and design was performed by Xiaotao Huang and Yingxing Xu. Data collection and analysis was performed by Chengshi Zou.

Acknowledgments

This study was funded by Zhejiang Cixi Science and Technology Planning Project (Granted number: CN2019022).

Conflict Of Interest

The authors declare that they have no competing interests.

References

1. Lasanianos NG, Garnavos C, Magnisalis E, Kourkoulis S, Babis GC. A comparative biomechanical study for complex tibial plateau fractures: nailing and compression bolts versus modern and traditional plating. Injury. 2013;44(10):1333–9. https://doi.org/10.1016/j.injury.2013.03.013

2. Rademakers MV, Kerkhoffs GM, Sierevelt IN, Raaymakers EL, Marti RK. Operative treatment of 109 tibial plateau fractures: five-to 27-year follow-up results. J Orthop Trauma. 2007;21(1):5–10. https://doi.org/10.1097/bot.0b013e31802c5b51

3. Biggi F, Di Fabio S, D'Antimo C, Trevisani S. Tibial plateau fractures: internal fixation with locking plates and the MIPO technique. Injury. 2010;41(11):1178–82. https://doi.org/10.1016/j.injury.2010.08.001
4. Prat-Fabregat S, Camacho-Carrasco P. Treatment strategy for tibial plateau fractures: an update. EFORT Open Rev. 2017;1(5):225–32. https://doi.org/10.1302/2058-5241.1.000031
5. Yoon RS, Liporace FA, Egol KA. Definitive fixation of tibial plateau fractures. Orthop Clin North Am. 2015;46(3):363–75. https://doi.org/10.1016/j.ocl.2015.02.005
6. Schatzker J. Tibial plateau fractures. In: Browner BD, Jupiter JB, Levine AM, et al., editors. Skeletal trauma. Fractures, Dislocations, Ligamenteous injuries. Volume 2. Philadelphia: WB Saunders; 1992. p. 1759.
7. Huang X, Zhi Z, Yu B, Chen F. Stress and stability of plate-screw fixation and screw fixation in the treatment of Schatzker type IV medial tibial plateau fracture: a comparative finite element study. J Orthop Surg Res. 2015;10:182. https://doi.org/10.1186/s13018-015-0325-2
8. Luo CF, Sun H, Zhang B, Zeng BF. Three-column fixation for complex tibial plateau fractures. J Orthop Trauma. 2010;24(11):683–92. https://doi.org/10.1097/bot.0b013e3181d436f3
9. Bryson WN, Fischer EJ, Jennings JW, Hillen TJ, Friedman MV, Baker JC. Three-column classification system for tibial plateau fractures: what the orthopedic surgeon wants to know. Radiographics. 2021;41(1):144–55. https://doi.org/10.1148/rg.2021200106
10. Chen P, Lu H, Shen H, Wang W, Ni B, Chen J. Newly designed anterolateral and posterolateral locking anatomic plates for lateral tibial plateau fractures: a finite element study. J Orthop Surg Res. 2017;12(1):35. https://doi.org/10.1186/s13018-017-0531-1
11. Favot LM, Berry-Kromer V, Haboussi M, Thiebaud F, Ben ZT. Numerical study of the influence of material parameters on the mechanical behaviour of a rehabilitated edentulous mandible. J Dent. 2014;42(3):287–97. https://doi.org/10.1016/j.jdent.2013.11.027
12. Högel F, Hoffmann S, Panzer S, Wimber J, Bühren V, Augat P. Biomechanical comparison of intramedullar versus extramedullar stabilization of intra-articular tibial plateau fractures. Arch Orthop Trauma Surg. 2013;133(1):59–64. https://doi.org/10.1007/s00402-012-1629-x
13. Ruedi TP, Buckley RE, Moran CG. AO Principles of Fracture Management. 2nd ed. Switzerland: AO Publishing; 2007.
14. Carrera I, Gelber PE, Chary G, González-Ballester MA, Monllau JC, Noailly J. Fixation of a split fracture of the lateral tibial plateau with a locking screw plate instead of cannulated screws would allow early weight bearing:a computational exploration. Int Orthop. 2016;40(10):2163–9. https://doi.org/10.1007/s00264-015-3106-y
15. Kutzner I, Heinlein B, Graichen F, Bender A, Rohlmann A, Halder A, et al. Loading of the knee joint during activities of daily living measured in vivo in five subjects. J Biomech. 2010;43(11):2164–73. https://doi.org/10.1016/j.jbiomech.2010.03.046